

## The Estimation of the Effective Centre of Mass Energy in $q\bar{q}\gamma$ Events from DELPHI

P. Abreu<sup>1</sup>, A. De Angelis<sup>2</sup>, G. Della Ricca<sup>3</sup>, D. Fassouliotis<sup>4</sup>, A. Grefrath<sup>5</sup>,  
N. Kjaer<sup>6</sup>, R.P. Henriques<sup>1</sup>, M. Mulders<sup>6</sup>, M. Pimenta<sup>1</sup>, L. Vitale<sup>3</sup>

### Abstract

The photon radiation in the initial state lowers the energy available for the  $e^+e^-$  collisions; this effect is particularly important at LEP2 energies (above the mass of the Z boson). Being aligned to the beam direction, such initial state radiation is mostly undetected. This article describes the procedure used by the DELPHI experiment at LEP to estimate the effective centre-of-mass energy in hadronic events collected at energies above the Z peak. Typical resolutions ranging from 2 to 3 GeV on the effective center-of-mass energy are achieved, depending on the event topology. *PACS codes: 07.05.K, 13.10.+q, 13.65.+i. Keywords: Data Analysis, Photon Radiation, Initial State Radiation.*

---

<sup>1</sup>LIP/FCUL/IST, Lisboa, Portugal

<sup>2</sup>CERN-CH 1211, Geneva, Switzerland

<sup>3</sup>INFN Trieste and Università di Trieste, Italy

<sup>4</sup>University of Athens, Greece

<sup>5</sup>University of Wuppertal, Germany

<sup>6</sup>NIKHEF, Amsterdam, The Netherlands

# 1 Introduction

The increase in the LEP beam energy above the Z in 1995 opened a new window of higher centre-of-mass (c.m.) energies to study  $e^+e^-$  annihilations. The Initial State Radiation reduces the energy available for the physical processes.

The photons from Initial State Radiation (hereafter called ISR photons) tend to move along the beam ( $z$ ) direction; thus, they are mostly undetected. Figure 1 shows the energy versus polar angle distribution of the ISR photon(s) in simulated hadronic events at a c.m. energy of 161 GeV. The initial  $q\bar{q}$  state was generated using the PYTHIA 5.4 [1] Parton Shower Monte Carlo. The polar angle,  $\theta$ , peaks at values close to zero, and the photon energies cluster at  $E_{\gamma R} = (s - M_Z^2)/(2\sqrt{s})$ , where  $s = (2E_b)^2$ ,  $E_b$  is the beam energy, and  $M_Z$  is the Z mass. For events with such a hard ISR, the energy in the c.m. of the  $e^+e^-$  collision is reduced to the Z mass (“Z radiative return” events).

This note explains the methods used by the DELPHI experiment at LEP to compute the effective centre of mass energy,  $\sqrt{s'}$ , in  $e^+e^-$  annihilations into hadrons, by measuring or estimating the energy and momentum of ISR photon(s). Two algorithms are used:

- the first one, based on the jet directions only, is more robust;
- the second, based on a constrained fit, is more precise.

The procedures described in this note were used in many papers from DELPHI (see for example [2, 3]). The DELPHI detector is described in [4], and its performance in [5].

## 2 The methods

One looks first for detected ISR photons. Showers unassociated to charged particles are searched for in the calorimeters, and they are considered as candidate ISR photons, if they fulfill the following criteria:

- energy deposition larger than 10 GeV;
- isolation angle larger than 0.3 radians with respect to any charged particle with momentum larger than 1 GeV;
- when the shower energy is smaller than 70 % of the photon energy corresponding to a radiative return to the Z, isolation angle with respect to any charged particle (with momentum larger than 1 GeV) larger than 0.6 radians and smaller than 1.5 radians (1.8 radians if the shower is contained in the small angle calorimeter, the STIC).

Showers are grouped together, if they are closer than 5 degrees in space. The association is done by adding the energies and assuming as direction the direction of the vector sum of the momenta.

### 2.1 Method 1: determination of the energy of ISR photon(s) from the direction of jets

The first method (called SPRIME inside the collaboration) uses only the direction of jets and of the detected photon(s) - if any.

All the particles in the event, except the one(s) considered as ISR photon(s) using the criteria described above, are forced to be clustered in two jets, using the DURHAM algorithm [6]. The particles are assumed to be massless.

The method applies energy and momentum conservation to estimate the energy of possible ISR photons lost along a direction close to the beam, after having considered the candidate one(s) directly detected in the electromagnetic calorimeters.

If no ISR photons are detected, an event plane containing the beam ( $z$ ) axis and maximizing the sum of the moduli of the projections of the jet momenta is determined. A hypothetical photon is assumed to be along  $z$ , in the positive or negative direction, respectively if the sum of the jet polar angles is larger or smaller than 180 degrees. The directions of the two jets, projected onto the event plane, are used to constrain the photon energy.

If only one ISR photon is measured in the detector and the event is planar, i.e., if the sum of the internal angles between the jets and the photon exceeds 345 degrees, the photon energy is calculated by energy-momentum conservation in the event plane containing the photon direction and maximizing the sum of the moduli of the projections of the jet momenta. For aplanar events at least one particle has been lost. The algorithm assumes that at another photon has been radiated inside the beam pipe and makes use of the energies of the jets and of the measured ISR photon to constrain the hypothetical photon energy.

If more than one ISR photon is measured, energy-momentum conservation is applied in the event plane to determine the energy of an unseen photon along  $z$  and the momenta of the two jets, using as an input the direction of the jets and the energies and the directions of the detected photons.

### 2.1.1 Results

The estimated effective c.m. energy ( $\sqrt{s'}$ ), for hadronic events (selected using the standard DELPHI hadronic criteria, see [7]) collected from the run around 188.7 GeV during 1998, is shown in the upper plot of figure 2 (data points) and is compared to a sample simulated with PYTHIA and followed through the complete simulation of the detector, DELSIM [5]. The results show a satisfactory description of the data by the simulation.

High efficiencies and purities are obtained for selecting “high energy” events (defined as those with effective energy above  $0.9\sqrt{s}$ ), and for selecting  $Z$  radiative return events. In the following, we shall call “low energy” events those with effective energy below  $0.9\sqrt{s}$ .

The generated effective c.m. energy for simulated events at beam energy of 80.5 GeV, selected requiring a SPRIME result above  $0.9\sqrt{s}$ , is shown in figure 3 (hollow histogram). The hatched histogram shows the same distribution for a subsample of those events in which the energy seen in the detector is above  $M_Z + (\sqrt{s} - M_Z)/2 = 126$  GeV. With this cut the small contamination due to events with effective c.m. energy near the  $Z$  mass is drastically reduced.

The efficiency to select high energy events was computed to be 88%, with a purity of the selected sample of 92%. When a larger purity is required, a cut on the total energy of the event may be applied. For the cut illustrated in the previous paragraph the purity was increased to 96%, with an efficiency of 74%.

Using simulated events with PYTHIA at c.m. energies of 130 GeV, 161 GeV and 188 GeV respectively, the efficiencies and purities for selecting “high energy” events, as

a function of the cut value in  $\sqrt{s'}/\sqrt{s}$ , are shown in figure 4.

Figure 5 shows the distribution of the low energy events, simulated at c.m. energy of 188 GeV, as a function of the difference between the SPRIME estimate and the generated effective energy. The Full Width at Half the Maximum (FWHM) of this distribution divided by 2.35 is used as an estimator of the resolution of SPRIME, and is shown on the left plot of figure 6 as a function of the DURHAM  $y_{cut}$  value needed to distinguish 2-jet from 3-jet events. The right plot of figure 6 shows the average offset of the method, defined as the peak value of the distribution of the difference between the SPRIME estimate and the generated effective energy.

## 2.2 Method 2: determination of the energy of ISR photon(s) from a constrained fit

The second method (referred to inside the collaboration as SPRIME+) uses a constrained fit taking into account the 4-momenta of the measured jets and photons and assuming one additional photon inside the beampipe. This method is able to include any number of jets and photons and is therefore more appropriate than the previous method in events with more than two jets. The fit also returns an estimated error on the effective c.m. energy, and a  $\chi^2$  indicating the goodness of the fit.

All particles that have not been identified as ISR photons are clustered into a “natural” number of jets using the DURHAM jet algorithm with a  $y_{cut}$  fixed to 0.002. This  $y_{cut}$  value was chosen to optimize the energy resolution; at this value, PYTHIA reproduces the data well.

Then two kinematical constrained fits are performed, corresponding to the hypotheses that an undetected photon went along the positive or negative z-direction (along the beam). There are two constraints from the transverse momentum balance,  $\sum p_x = 0$  and  $\sum p_y = 0$ , and one from conservation of the total energy and of the momentum along the beam direction:

$$\sum E = \sqrt{s} - \sum p_z \quad \text{or} \quad \sum E = \sqrt{s} + \sum p_z$$

assuming  $\sum p_z > 0$  or  $\sum p_z < 0$  respectively.

The fitted jet momentum,  $\vec{p}_j^f$ , was projected onto a set of axes with one component parallel to the measured jet momentum,  $\vec{p}_j^m$ , and two transverse components. The parallel component was described by a rescaling factor,  $\exp(a_j)$ , while the transverse components were described by parameters multiplying perpendicular momenta fixed to 1 GeV/c:

$$\vec{p}_j^f = \exp(a_j)\vec{p}_j^m + b_j\vec{p}_j^b + c_j\vec{p}_j^c.$$

To determine  $\vec{p}_j^b$  and  $\vec{p}_j^c$ , the jet energy,  $E_j^m$ , and thereby also to a good approximation the jet mass, was rescaled with the same factor  $\exp(a_j)$  as the jet momentum; the fitting algorithm then minimized a  $\chi^2$ :

$$\chi^2 = \sum_j \frac{(a_j - a_0)^2}{\sigma_{a_j}^2} + \frac{b_j^2}{\sigma_{b_j}^2} + \frac{c_j^2}{\sigma_{c_j}^2},$$

while forcing the fitted event to obey the constraints.

The errors were parametrized as a function of the polar angle  $\theta_j$  of the jet with respect to the beam:

$$\begin{aligned} a_0 &= 0.15 + 0.40 \cdot \cos^4\theta_j \\ \sigma_{a_j} &= 0.15 + 0.40 \cdot \cos^4\theta_j \\ \sigma_{b_j} = \sigma_{c_j} &= 1.8 + 1.08 \cdot \cos^4\theta_j \text{ GeV} \end{aligned}$$

Photons are treated in the same way as jets, but with smaller estimated measurement errors:

$$\begin{aligned} a_0 &= 0 \\ \sigma_{a_j} &= 0.04 \\ \sigma_{b_j} = \sigma_{c_j} &= 0.01 \text{ GeV} . \end{aligned}$$

When, after the fit,  $\sum p_z$  has the same sign as assumed in the constraints, the solution is said to be “physical”, otherwise it is called “unphysical”. The solution is chosen that has the smallest  $\chi^2$  and is physical. If both solutions are unphysical the measured energy and momentum balance indicate that there was no significant photon lost inside the beampipe. In that case a new constrained fit is performed, using the four constraints of momentum and energy conservation with  $\sum p_z$  fixed to zero.

The fitting algorithm used is similar to the method described in detail in [3].

In case the standard fit as described above does not converge, a special procedure is applied to try to recuperate the event. The longitudinal errors are relaxed for the measured jets:

$$\begin{aligned} a_0 &= 0.75 + 2.0 \cdot \cos^4\theta_j \\ \sigma_{a_j} &= 0.75 + 2.0 \cdot \cos^4\theta_j \end{aligned}$$

and for the photons:

$$\begin{aligned} a_0 &= 0 \\ \sigma_{a_j} &= 0.057. \end{aligned}$$

Then a series of fits is done with the 4 constraints of energy and momentum conservation after assuming an additional photon along  $z$ , with momentum  $p_z = -100, -95, -90 \dots +95, +100$  GeV along the beam.

The fit with the smallest  $\chi^2$  is chosen. If there are at least three fits around the minimum that converged, interpolation with a parabola is used to improve the determination of the  $p_z$  with the lowest  $\chi^2$ . A final fit is done with  $p_z$  constrained to this value.

### 2.2.1 Results

The performance of the constrained fit method was studied using PYTHIA  $q\bar{q}\gamma$  simulation at c.m. energies of 130 GeV, 161 GeV and 188 GeV, including the full detector simulation DELSIM.

The constrained fit turns out to be quite robust. The standard fit does not converge in 0.4% of the events, in which case the recuperation method is used. This method is able to recuperate 60% of the events that failed.

The resolution obtained with SPRIME+ can be seen from Figure 5. The improvement in resolution and offset with respect to SPRIME is evident especially for events with a high  $y_{cut}$  from 3 to 2 jets, for which the assumption of 2 massless jets is no longer valid (at a c.m. energy of 161 GeV, 46% of the events have  $y_{cut} > 10^{-3}$ ). This is shown for the reconstruction of Z radiative return events in figure 6.

The improvement in resolution leads to higher efficiencies for selecting events with  $\sqrt{s'}$  larger than  $0.9\sqrt{s}$  (figure 4). For very high purities, however, there is hardly any improvement. This is due to a side effect of the improved resolution for 3-jet like configurations: when an energetic ISR photon is radiated inside the detector acceptance but not tagged as an ISR photon, it is treated as a third jet in SPRIME+, giving an estimated effective c.m. energy larger than  $0.9\sqrt{s}$ . As SPRIME has a worse resolution for 3-jet like events, a significantly larger part of events of this type miss the cut, resulting in a higher purity.

With a cut requiring SPRIME+ larger than  $0.9\sqrt{s}$ , the efficiency and purity for events with generated  $\sqrt{s'}$  larger  $0.9\sqrt{s}$  for the PYTHIA MC sample at 161 GeV are 94% and 90% respectively.

In figure 2 the data taken at 189 GeV is compared to simulation. The high energy peak is well separated from the radiative return peak. The figure also shows the improved resolution for the background which mainly consists of W pair events. The multi-jet events coming from the fully hadronic decay are reconstructed very well at the full c.m. energy. The large tail at low  $\sqrt{s}$  consists of hadronic-leptonic and fully leptonic W pair events containing neutrinos that are not included in the reconstruction hypothesis.

### 3 Summary

The methods used by DELPHI for the determination of the effective center-of-mass energy in hadronic events at LEP 2 were presented.

The “high energy” peak is very well separated from the radiative return to the Z, allowing for efficiencies and purities well above 80% to be obtained for selecting events with effective energy greater than  $0.9\sqrt{s}$  (“high energy” events) or in the region of the Z mass (“Z radiative return” events).

Typical resolutions ranging from 2 to 3 GeV on the effective center-of-mass energy are achieved, depending on the event topology.

### Acknowledgements

We would like to thank the colleagues from the DELPHI collaboration, who tested the algorithms presented in this paper helping to improve them. We thank in particular W. Venus for reading and commenting the manuscript.

## References

- [1] T.Sjöstrand, Comp. Phys. Commun. **82** (1994) 74.
- [2] DELPHI Coll., P. Abreu et al., Phys.Lett. **B372** (1996) 172;  
DELPHI Coll., P. Abreu et al., Z. Phys. **C73** (1997) 229;  
DELPHI Coll., P. Abreu et al., Phys. Lett. **B397** (1997) 158;  
DELPHI Coll., P. Abreu et al., Phys. Lett. **B401** (1997) 181;  
DELPHI Coll., P. Abreu et al., Phys. Lett. **B416** (1998) 233.
- [3] DELPHI Coll., P. Abreu et al., Eur. Phys. J. **C2** (1998) 581.
- [4] DELPHI Coll., P. Aarnio et al., Nucl. Instr. and Meth. **A303** (1991) 233.
- [5] DELPHI Coll., P. Abreu et al., Nucl. Instr. and Meth. **A378** (1996) 57.
- [6] S. Bethke et al., Phys. Lett. **B213** (1988) 235.
- [7] DELPHI Coll., P. Abreu et al., “Measurement and Interpretation of Fermion-Pair Production at LEP energies from 130 to 172 GeV”, *in preparation*.

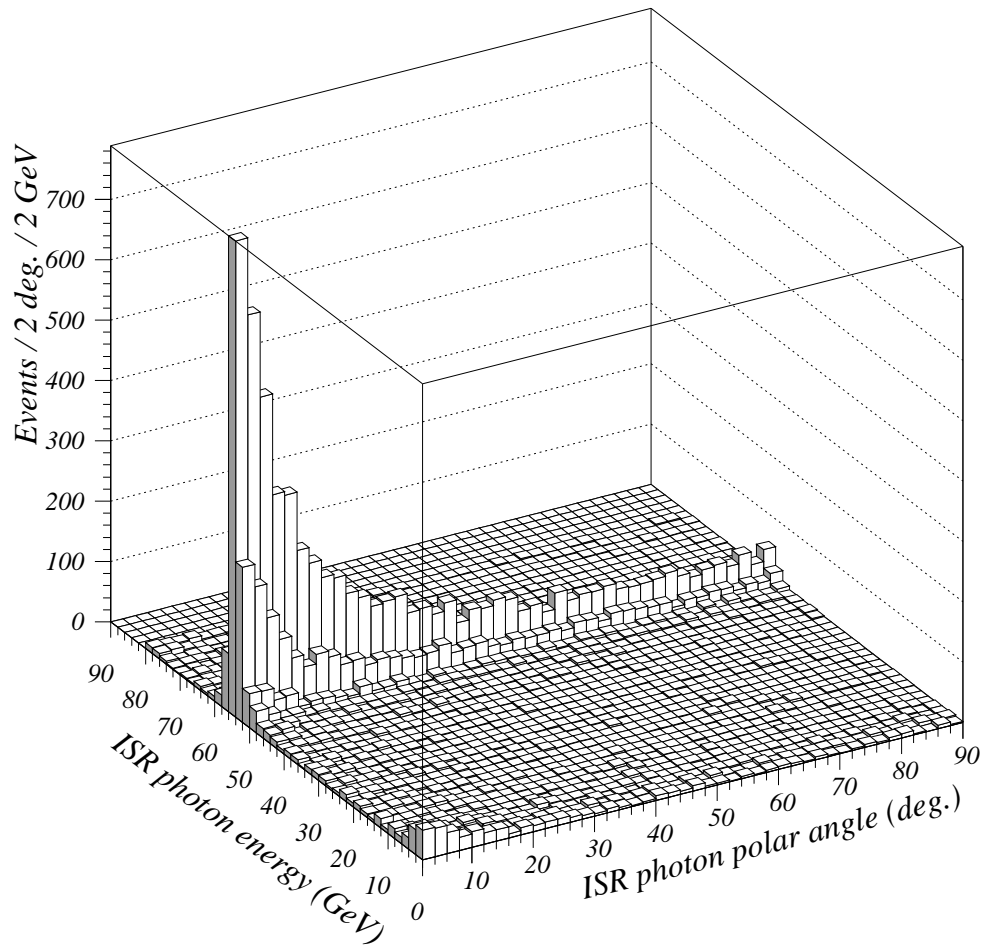


Figure 1: Energy as a function of polar angle for ISR photons at c.m. energy of 161 GeV. Photons below 2 degrees are not plotted.



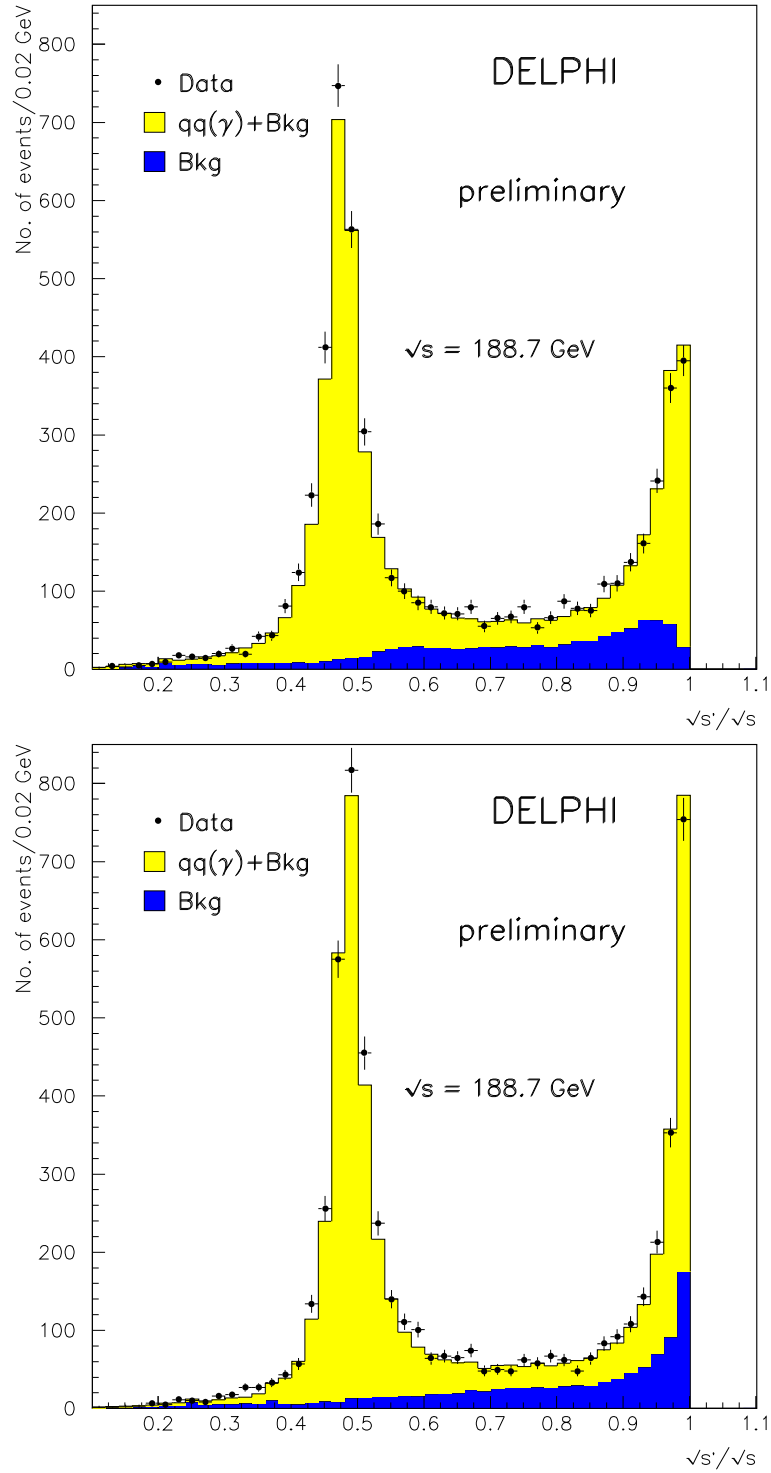


Figure 2: SPRIME (top) and SPRIME+ (bottom) results for the data collected during early 1998 at a c.m. energy around 188 GeV (black bullets), compared to the simulated events at the same energy using PYTHIA. The data correspond to an integrated luminosity of about  $54 \text{ pb}^{-1}$ .

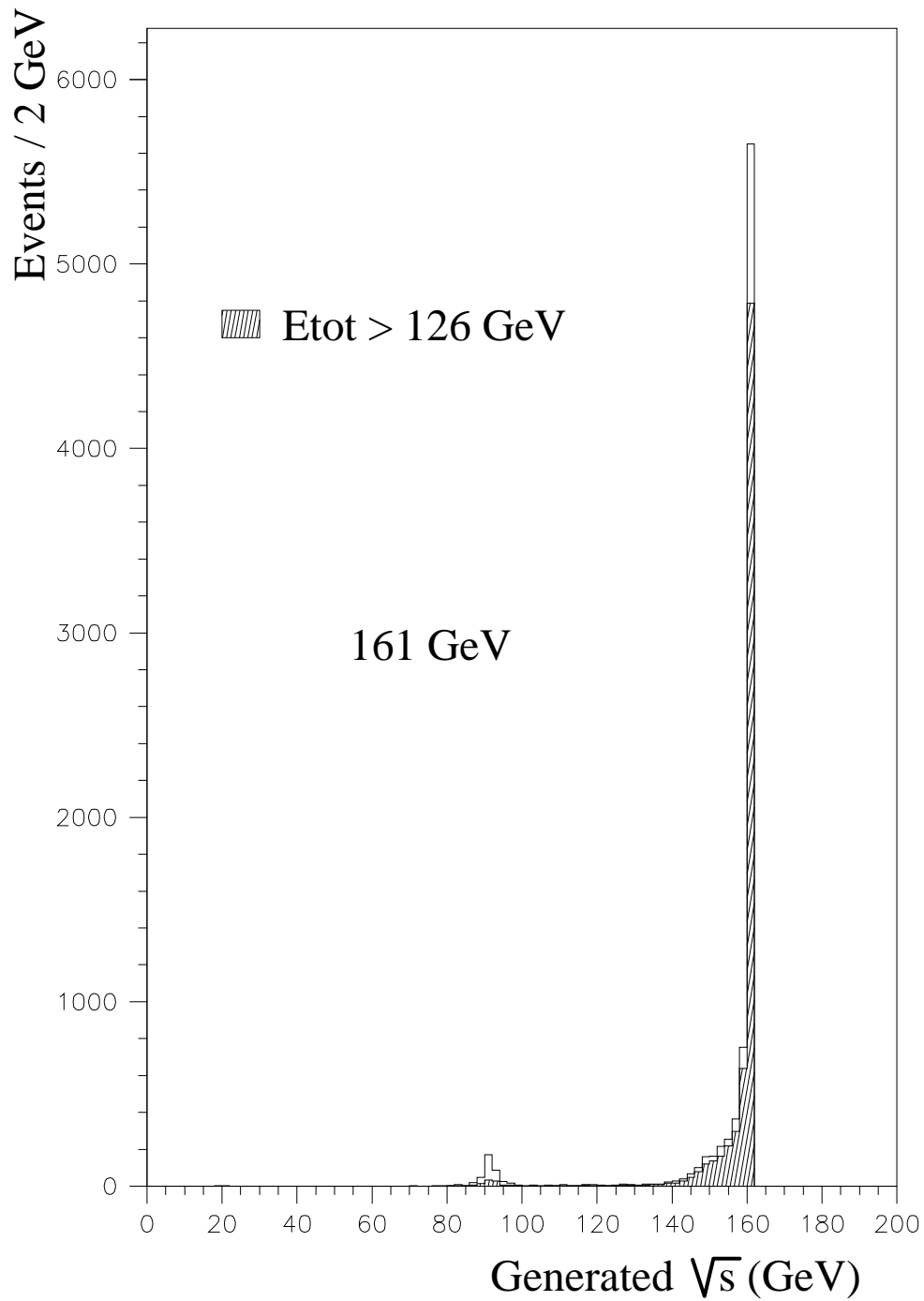


Figure 3: Generated effective centre of mass energy for simulated events with a SPRIME result above  $0.9\sqrt{s}$  (solid line), and the same distribution for events with a SPRIME result above  $0.9\sqrt{s}$  and requiring that the total energy seen in the event is above 126 GeV.

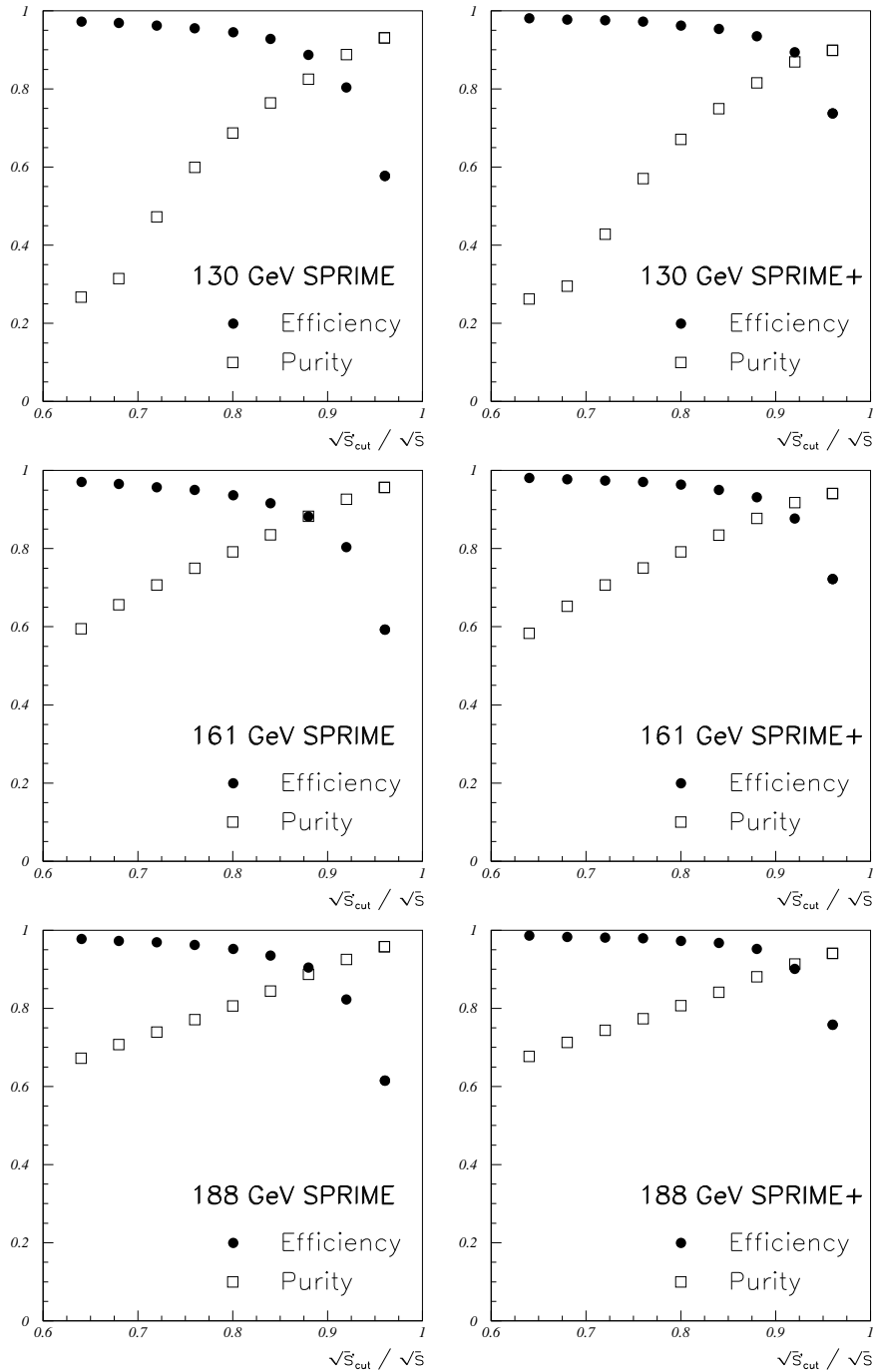


Figure 4: Efficiency (black bullets) and purity (white squares) for selecting events with generated effective centre of mass energy above  $0.9\sqrt{s}$  as a function of the cut applied on the ratio of the SPRIME (left) or SPRIME+ (right) result to the LEP c.m. energy. The results are shown for simulated events at c.m. energies of 130 GeV (two upmost plots), 161 GeV (two central plots) and 188 GeV (two lowmost plots).

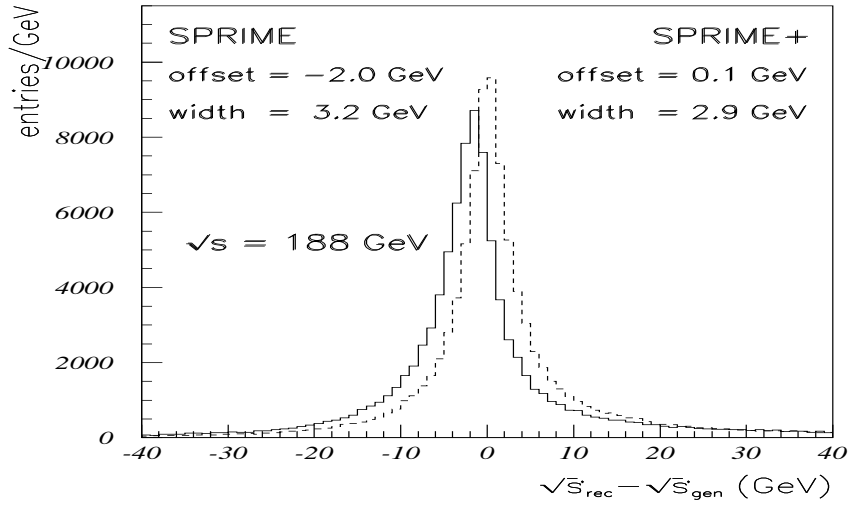


Figure 5: Solid line: distribution of PYTHIA simulated events at an energy in the centre of mass of 188 GeV as a function of the difference between the SPRIME result and the generated effective c.m. energy. Dashed line: same for SPRIME+.

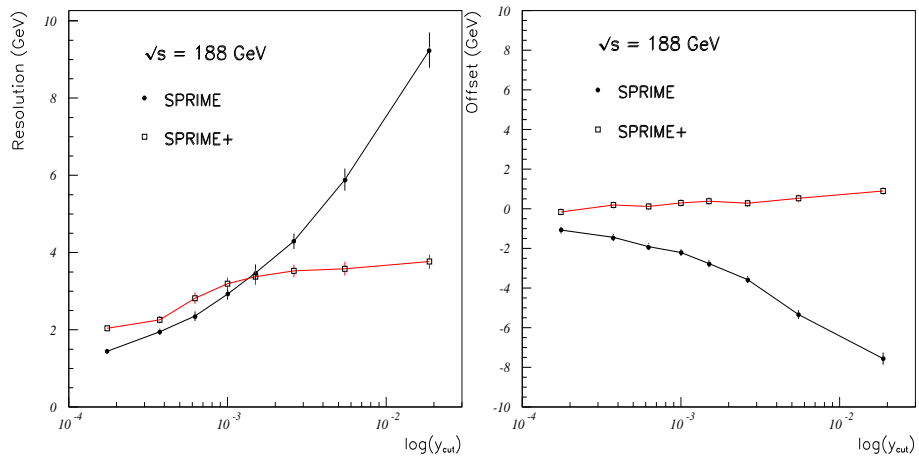


Figure 6: Left: Resolution of SPRIME and SPRIME+, as a function of the minimal  $y_{cut}$  needed for DURHAM to reconstruct two jets. Right: Average offset for SPRIME and SPRIME+, as a function of  $y_{cut}$ .